

## **Integrated Modelling of ITER Plasma Dynamics and Wall Processes Following Type I ELMs and Consequences for Tokamak Operation**

I.S. Landman 1), S.E. Pestchanyi 1), G. Janeschitz 1), V.M. Safronov 2),  
Y. Igitkhanov 1), B.N. Bazylev 1)

1) Forschungszentrum Karlsruhe, IHM, FUSION, P.O. Box 3640, 76021 Karlsruhe, Germany

2) State Research Centre TRINITI, 142190, Moscow Region, Troitsk, Russian Federation

E-mail contact of main author: [igor.landman@ihm.fzk.de](mailto:igor.landman@ihm.fzk.de)

**Abstract:** The anticipated regime of ITER is the H-mode in which the ELMs can significantly deteriorate the operation. The lost plasma is dumped into the SOL and then impacts on the target producing sputtering and vaporization erosion. The following contamination of core plasma by eroded atoms can interrupt the confinement. For tokamak modelling with account for the transients, the tokamak geometry MHD codes FOREV and TOKES have been developed. The FOREV models the processes on the time scale of 1 ms with the CFC wall. The modelling for ITER plasma evolution following the carbon influxes revealed that significant impurity contamination of the edge plasma can occur, which can cause large radiation losses and eventually lead to the collapse of the confinement at lesser ELM sizes than that determined by armour lifetime limitations. The TOKES is developed for the integrated simulation on the discharge scale ( $10^3$  s), however permitting multiple ELMs. Multi-fluid plasma and corona radiation transport are implemented. In the modelling for ITER with B-C-W wall, the scattered atoms have significant chances to strike secondarily the dome and thus produce sputtered W-atoms even with the CFC wall at the separatrix strike point. The ELMs cause untimely discharge interruption if the ELM energy exceeds the vaporization onset. To validate the codes, dedicated experiments have been carried out. CFC targets manufactured for ITER have been exposed at the plasma gun MK-200UG in TRINITI. On the basis of these experiments, significant plasma contamination is expected for ITER transients at the target heat deposition above  $0.5 \text{ MJ/m}^2$ , which corresponds to the vapour shield threshold and agrees with the FOREV and TOKES simulations.

### **1. Introduction**

The anticipated regime of the tokamak ITER is the H-mode in which the repetitive outbreaks of the edge-localized mode (ELM) with the duration  $\sim 0.5$  ms can significantly influence the operation. On the basis of scaling from present experiments [1,2], the ELM induced energy deposition at the divertor armour can reach up to several  $\text{MJ/m}^2$ . The lost plasma is dumped into the scrape-off layer (SOL), propagates along the magnetic field lines and impacts on the target producing surface erosion by sputtering and vaporization. The following contamination of core plasma by eroded atoms can deteriorate the confinement and even cause a disruption.

For the ITER loads the computer simulations are developed in FZK aiming mainly at the transients, and experimental studies for models validations are carried out in TRINITI [3]. Here mainly the current state of computer modelling is described. It follows from the coupling of involved plasma and wall processes that adequate modelling for modern tokamaks needs implementing in one code multi-species plasma transport both across the confinement region and along the magnetic field lines ending at the vessel walls, as well as account of diverse events at the vessel surface in order to establish appropriate boundary conditions for the plasma. Thus numerical algorithms valid in the whole vessel have to be developed. The intermittent particle and energy flows have to be calculated both for plasma and neutral atoms, taking into account the transport of electromagnetic radiation.

For the modelling of plasma contamination following the transients the tokamak geometry MHD codes FOREV and TOKES have been developed. The FOREV (Fig. 1) models the processes on the time scale of 1 ms assuming the CFC wall. It calculates the vapour shield

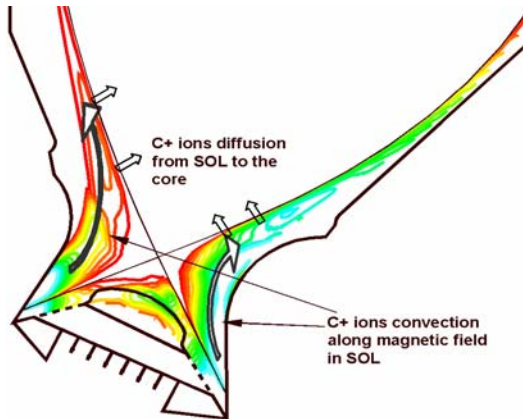


FIG. 1: FOREV: Transport of C-ions in the ITER vessel: the red colour corresponds to a minimum ion density  $n_{min}$ , cyan – to the maximum  $n_{max}$  that can reach  $3 \times 10^{22} \text{ m}^{-3}$ .

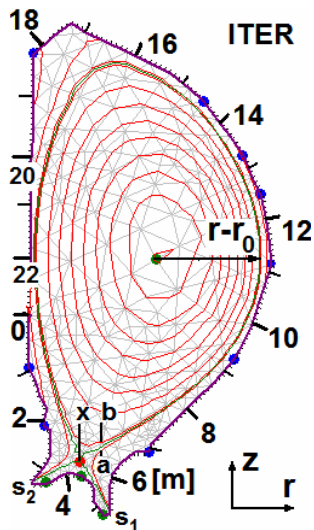


FIG. 2. The ITER poloidal layout in TOKES with the triangular meshes, the magnetic flux coordinates and the wall coordinate  $X$ .

that develops in front of ITER divertor surface protecting it after strong ELMs and during the disruptions and the following propagation of eroded ionized carbon into the SOL and the edge of confined plasma. The TOKES (Fig. 2) was recently developed for the integrated simulation on the discharge scale ( $10^3 \text{ s}$ ) with nominal time step of a few ms, however permitting multiple ELMs during which the time step gets as small as necessary. In this code the magnetic field can evolve together with the confined plasma, because the currents are recalculated after each time step. Poloidal field coils (not shown) automatically control plasma shape. The Pfirsch-Schlüter multi-fluid plasma model with the gyro-Bohm cross-diffusion and

thermal conduction are implemented so far. The fluids are ionized plasma species from hydrogen isotopes to tungsten of different charge states and bound electron excitation states. The detailed species description in the confinement region allowed implementation of corona model including ionization equilibrium. The SOL transport is implemented based on the guiding centre model for the ions.

For validation of FOREV a dedicated research has been developed in frame of FZK-TRINITY collaboration. CFC targets manufactured in EU for ITER divertor armour have been exposed to pulsed magnetized hydrogen streams at the plasma gun MK-200UG, with the pulse duration 0.05 ms, ion energy 2.5 keV and in leading magnetic field up to 2.5 T [3]. Radiation properties of evaporated carbon were studied near the target surface up to the distance of 15 cm. The multiple ionization of carbon ions, their temperature, density and velocity have been measured as functions of plasma load.

## 2. FOREV modelling of plasma contamination

During a disruption the heat flux  $q$  on the target surface increases drastically compared to that of ELM. However, the surface impact gets limited due to a vapour shield that forms from eroded and ionized material close to SSP. A large fraction of impacting energy is reradiated by the vapour shield carbon plasma onto the structures surrounding the divertor. The carbon expands into SOL and then penetrates into the confinement region. As a consequence, the thermal energy of confined plasma is reradiated onto the first wall directly from the pedestal. In FOREV scenario simulating this process (see Fig. 1) the loss of confinement is assumed due to a drastic increase of plasma cross-diffusion coefficient  $D_{\perp}$ , fitting its magnitude to the fluxes from  $q = 30$  to  $130 \text{ GW}$ .

After disruption onset,  $D_{\perp}$  grows linearly during 0.2 ms and then it remains constant for 3 ms. Target vaporization starts from 0.06 ms ( $q = 130$ ) to 0.2 ms ( $q = 30$ ). The carbon expanding in SOL has varying densities of  $10^{21} - 10^{22} \text{ m}^{-3}$  that depend on  $q$ . However,  $q$  weakly changes the

carbon temperature limited by a few eV, because the energy is immediately converted into the radiation ('radiation barrier'). As the result, at the divertor target the flux reduces getting about  $10^{-2}q$  but it keeps a small vaporization rate. The SOL carbon plasma crosses the separatrix in vicinity of the x-point and also diffuses to the first wall. In the pedestal the

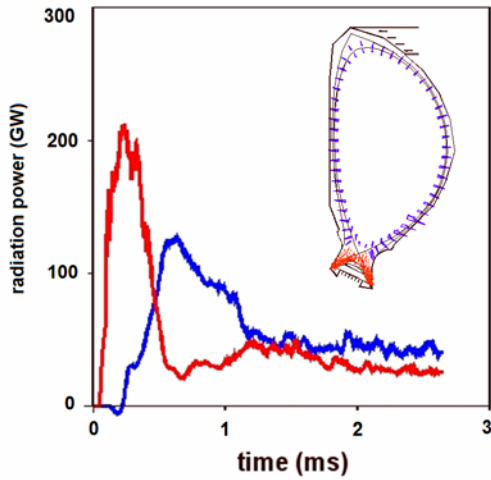


FIG. 3: Simulated radiation power from the divertor region (in red) and the core (blue) for a disruption with  $q = 63$  GW.

carbon inflow causes fast radiation cooling of confined plasma. The time dependence of radiation power from the divertor region, in comparison with that from the pedestal, is shown in Fig. 3. The disruptions with smaller  $q$  produce radiation mainly from the divertor region and increasing  $q$  leads to larger radiation losses from the pedestal. At  $q = 130$  GW the pedestal losses reach 85%. The pedestal plasma is eventually cooled down to a few eV and the confinement terminates within 3 ms.

For ELMs, the FOREV simulations revealed that the vaporization at the divertor plate can be described in a simplified way, which saves considerably the CPU time. This model uses the result that the plasma shield temperature is not

sensitive of  $q$ . The simulations for ELMs with the shielding showed that after the vaporization onset followed by a short transition period the vaporization rate  $r_{\text{vap}}$  becomes almost constant during 0.15 - 0.18 ms, and  $r_{\text{vap}}$  depends only on the heat flux increase rate  $\dot{G}$  of ELM. Pre-surface carbon density becomes also approximately constant. As the result, maximum vaporization depth  $h_{\text{vap}}$  after e.g. one ELM of the duration  $\tau = 0.5$  ms saturates at increasing  $\dot{G}$  at  $h_{\text{vap}} \approx 6.5$   $\mu\text{m}$ . As  $h_{\text{vap}}$  the vaporization area increases with increasing  $\dot{G}$ , the vaporized amount  $N_{\text{vap}}$  does not saturate. The following analytical formula fits well calculated dependence of  $r_{\text{vap}}$  on  $\dot{G}$ :

$$r_{\text{vap}}[\text{atom}/\text{m}^2\text{s}] = 1.5 \cdot 10^{27} \ln(\dot{G}/\dot{G}_0), \quad \dot{G} \geq \dot{G}_0, \quad \dot{G}_0 = 0.15 \times 10^5 \text{ GW}/\text{m}^2/\text{s}$$

For example, at the ELM deposition energy  $1.8 \text{ MJ}/\text{m}^2$ , which corresponds to  $\dot{G} = 0.27 \times 10^5 \text{ GW}/\text{m}^2/\text{s}$  and  $\tau = 0.5$  ms, evaporated amount follows as  $N_{\text{vap}} = 0.88 \times 10^{23} \text{ m}^{-2}$ .

### 3. Experiments at MK-200 UG and FOREV validation

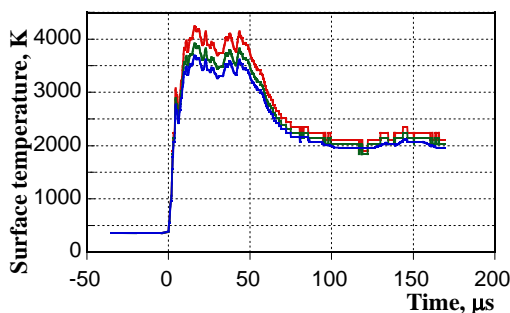


FIG. 4: Surface temperature of CFC target evaluated for surface emissivity 1 (in blue), 0.8 (green) and 0.6 (red);  $q = 0.24 \text{ MJ}/\text{m}^2$ .

The MK-200UG reproduces such parameters of ITER ELMs as the energy flux, impact ion energy, plasma density and pressure. The CFC NB31 was tested under the heat fluxes of varying magnitude. The samples have a flat rectangular shape with a face surface  $2.5 \times 2.5$  cm and the thickness 1 cm. To measure the absorbed energy, the targets are equipped by thermocouples. The surface temperature  $T_s$  is measured by a pyrometer with time resolution 0.1  $\mu\text{s}$ . For analyses of evaporated carbon, visible (4000-7000Å) and EUV (10-400Å) spectrometers with space resolution of 0.1 cm were applied [3].

For evaluation of CFC thermal conductivity,  $\lambda$ , flux threshold of CFC evaporation has been measured and then compared with FOREV value [4]. Also the vapour shield threshold was experimentally detected. A weak evaporation occurs already at  $q \sim 0.15 \text{ MJ/m}^2$  ( $T_s \approx 3000 \text{ K}$ ) and at  $q \approx 0.2 \text{ MJ/m}^2$  ( $T_s \approx 4000 \text{ K}$ ) intense evaporation starts. With further increase of  $q$ ,  $T_s$  remains unaltered, which indicates that the vaporization threshold equals  $0.2 \text{ MJ/m}^2$ . Fig. 4 presents  $T_s$  measured by the pyrometer at  $q = 0.24 \text{ MJ/m}^2$ . These measurements confirm also the threshold  $0.2 \text{ MJ/m}^2$ . At  $q = 0.2 - 0.3 \text{ MJ/m}^2$  the carbon plasma consists of  $\text{C}^{+1} - \text{C}^{+5}$  ions reaching the temperature  $10 - 30 \text{ eV}$ . The density of C near the surface is  $n_C = 2 \times 10^{23} \text{ m}^{-3}$ , and C propagates along the magnetic field with a velocity  $1 - 2 \times 10^4 \text{ m/s}$  and  $n_C > 10^{21} \text{ m}^{-3}$ .

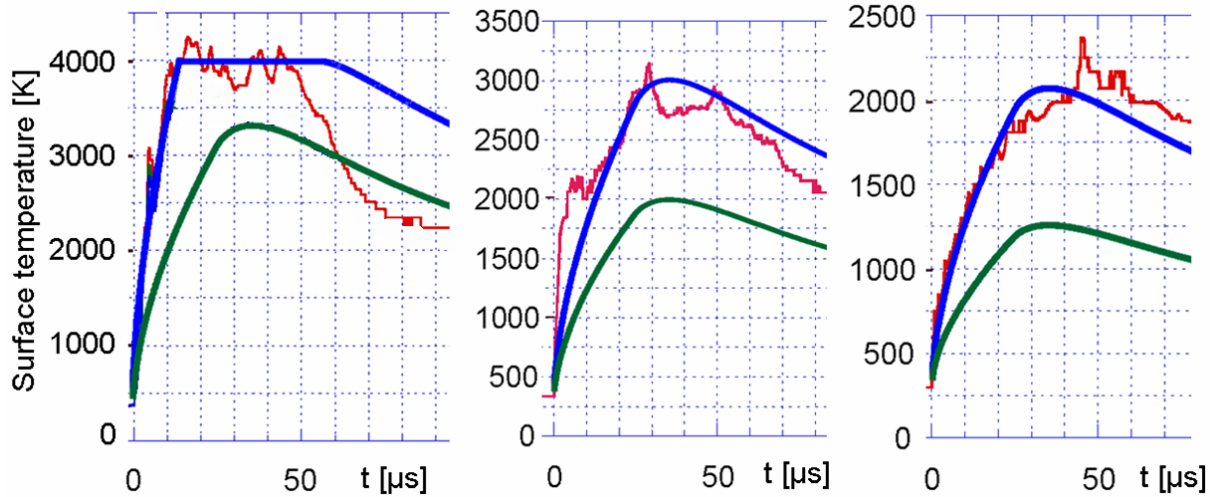


Fig. 5. Measured and simulated surface temperature  $T_s$  for  $q = 0.24 \text{ MJ/m}^2$ ,  $0.145 \text{ MJ/m}^2$  and  $0.09 \text{ MJ/m}^2$  are shown, in respect of the plots. The lower numerical curve of  $T_s$  (in green) corresponds to  $\lambda \approx \lambda_{ref}$  and the other (blue) to  $\lambda \approx 0.35\lambda_{ref}$ .

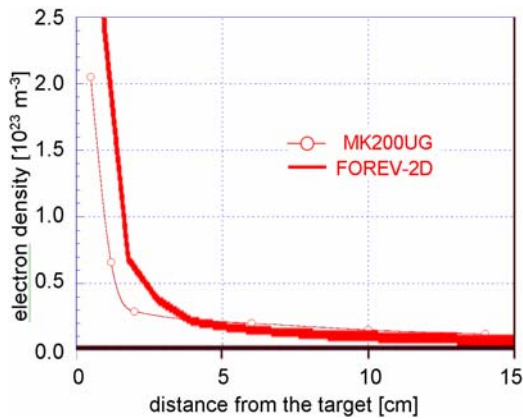


FIG. 6: Comparison of measured and simulated space distribution of electron density in front of CFC target at  $13 \mu\text{s}$ .  $q = 0.3 \text{ MJ/m}^2$ ,  $\lambda = 0.35\lambda_{ref}$ .

Comparison of measurements for the CFC target with respective FOREV simulations revealed that the numerical results are incompatible with the reference thermal conductivity  $\lambda_{ref}$  of NB31 used in the calculations. However, if assuming  $\lambda \approx \lambda_{ref}/3$  at all temperatures, the disagreement significantly decreases. It seems that after a hundred of severe thermal shocks the CFC fibres get significantly degraded due to the brittle destruction on the depth of  $0.1 - 0.2 \text{ mm}$ . Therefore the contradiction is attributed to a thin pre-surface layer of few hundred  $\mu\text{m}$  which was damaged by the previous impacts. As to the CFC bulk, it can have  $\lambda \approx \lambda_{ref}$ . For stationary heating regime, the temperature drop across the damaged layer is small compared to bulk

temperature drop. In this case  $\lambda_{ref}$  determines the thermal transport. But during the fast heating on the time scale  $0.1 \text{ ms}$  only the pre-surface layer participates in the transport, which can significantly decrease involved  $\lambda$  if the surface is damaged. The measured and simulated surface temperature and plasma shield densities at  $10 - 15 \mu\text{s}$  and the distance  $1 \text{ cm}$  from the surface are shown in Figs. 5 and 6. Thus by fitting  $\lambda$  a good agreement between the measured and the calculated electron density and surface temperature was finally achieved.

#### 4. TOKES development for integrated simulations of ITER ELMy H-mode

The new TOKES features include the gyro-Bohm transport model that takes account of neo-classical effect and allows controlled fusion power and feedback on the beam heating, and a plasma impact model based on the guiding centre approximation for the ions lost through the separatrix and then guided to vicinity of SSP (marked with “s<sub>1</sub>” and “s<sub>2</sub>” at Fig. 1) [5]. Either the W-divertor or that with the replacements of W by two CFC-armour fragments at  $X = (2.8-3.4)$  and  $(5.3-5.9)$  m was simulated. For the first wall ( $X < 2$  and  $X > 7$  m) Be-armour is set.

In TOKES simulations for the fusion gain 10 without the ELMs, the CFC surface temperature remains below the vaporization point. In this case the physical sputtering erosion and the backscattering are taken into account. At the impact the ions are assumed to recombine. The atoms scattered from the SSP have significant chances to strike secondarily the dome and thus produce sputtered W-atoms even with the C-wall at SSP. There is no unlimited contamination: the impurity densities remain limited as  $n_W < 5 \times 10^{15} \text{ m}^{-3}$ ,  $n_C < 3 \times 10^{16} \text{ m}^{-3}$  and  $n_{Be} < 2 \times 10^{15} \text{ m}^{-3}$ , which is attributed to the entrainment of impurities by the outflow of D- and T-ions fuelled (by equal amounts) into the confinement region. The heat outflow from the plasma reaches 82 MW and the radiation losses 5 MW. These losses are balanced by the fusion power of  $\alpha$ -particles and the beam power 30 MW. The surface maximum temperature exceeded 3000 deg(K). In current regime of TOKES simulations the separatrix temperature  $T_S$  is about 1.5 keV. Thus all involved species but W-impurity are fully ionized. For a Be-C-W wall at the discharge time  $t = 150$  s the bremsstrahlung load is obtained to be rather small ( $11 \text{ kW/m}^2$ ) and thus a small surface temperature rise due to radiation follows (about 10 deg).

The ELMs as simulated with TOKES can cause untimely discharge interruption. To estimate the range of tolerable ELMs, the ELM energy  $W_{ELM}$  (MJ) was varied in a wide range keeping for the ELM duration  $\tau_{ELM} = 0.3$  ms. Based on the simulations with the C-fragments, at  $4 < W_{ELM} < 15$  the termination time is approximated as  $t_{max}(s) \approx 3 \times (15 - W_{ELM})^2 / (W_{ELM} - 4)^2$ . At  $W_{ELM} < 4$ ,  $t_{max} = \infty$  is obtained, and at  $W_{ELM} > 15$  the termination occurs immediately after reaching the vaporization temperature 4100 K during the first ELM. Our attempt to solely replace the C-fragments by the W-wall resulted in immediate termination of even ELMy-free discharge within one second caused by drastic increase of tungsten density in the confinement region. Fig. 7 demonstrates the behaviour of  $n_W$  and  $T_W$  when after reaching the steady state equilibrium with the Be-C-W wall, C was suddenly replaced by W at the moment 200 s. During the discharge decay time  $\Delta t$  the radiation flux increases drastically, reaching in the maximum about 1 GW at  $\Delta t = 0.1$  s and then dropping down to 0.1 GW at  $\Delta t = 0.5$  s. It is

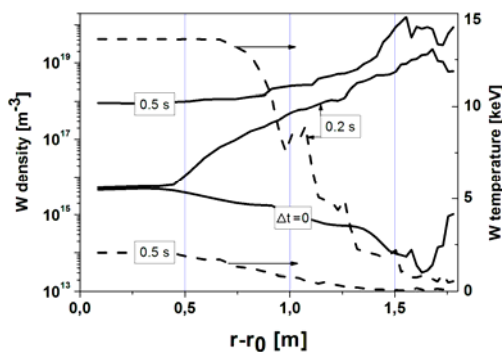


FIG. 7. The decay of discharge after replacement of C-fragment by W wall with the indicated time intervals after the moment 200 s.

concluded that the reason of the abrupt contamination is the development of W self-sputtering at high  $T_S$  because of acceleration of impacting ions in the pre-surface sheath up to 4.5 keV. According to the TOKES database, the sputtering yield  $Y_{WW}$  at the impact energy of W ions 4.5 keV reaches  $Y_{WW} \approx 3$ . Within  $\Delta t \sim 10^{-2}$  s the W sputtering becomes due to the W impurity coming from the hot plasma.

The new TOKES model for ion populations  $N_{mzk}$  and radiation transport is described in [6], with  $m$  the isotope index from H, D, T to W,  $z$  the charge state and  $k$  the level index. The  $N_{mzk}$  are

calculated along with  $T_e$  and the transition rates among level energies  $E_{mzk}$ . The photon absorptions and emissions are described in terms of opacities, which are emission coefficients  $\beta$  and absorption coefficients  $\kappa'$  that include spontaneous and induced radiation. The database of TOKES contains also the oscillator strengths  $f_{mzkk'}$  and the transition frequencies  $\nu_{mzkk'}$  for resonance excitations and  $\nu_{mzk}$  for the ionizations of atoms and ions by electron and photon collisions, which was collected using diverse sources and approximations. The ground state ionization potentials  $I_{nz} = E_{m,z+1,0} - E_{m,z,0}$  (with  $n$  the chemical number of isotope  $m$ ) are available for all  $m$  and  $z$ , but only the frequencies of the transitions from ground state to excited states of neutral atoms ( $z = 0$ ) are usually known. Therefore for ions ( $z > 0$ ) the scaling laws [7] on the ratios  $I_{n+z,z}/I_{n0}$  are applied along the isoelectronic sequences  $n-z = \text{const}$ . The atomic data on resonance transitions is taken from a free access database [8], but much is missing there even at  $z = 0$ . The lacking data of chemical numbers  $n'$  is obtained by some extrapolations from available numbers  $n$ . The complexity of atomic data prevents in reality direct multi-species self-consistent radiation transport simulations therefore in TOKES the data is reduced and approximated grouping the energy levels.

This radiation-population model is developed so far only for the confined plasma. As to the plasma dumped into SOL across the separatrix, it is still represented by fully ionized ions and their energies [6,9]. To the latter, the electron thermal energy proportionally to their charge state and the internal energy of plasma ions are added. The radiation losses from SOL are not yet implemented. An ion  $m$  impacting on the wall brings the full energy that contains a) the contribution of electrons, which the ion gains in reality when crossing the electric sheath in front of the wall, and b) the recombination contribution (because the ion internal energy would be released at the wall surface). The ions emerging in the SOL are grouped in some bunches, and a bunch is simulated in the guiding centre approximation. The passing times  $\tau_i$  through each triangle become available and then averaged ion densities  $\bar{n}_i$  in each triangle. The atomic rays that cross the triangles are treated similarly, obtaining corresponding averaged parameters  $\bar{n}_a$  and  $\bar{T}_a$  required for the calculation of atom-ion interactions. In SOL the ionization and the charge-exchange processes are preliminary simulated prescribing the SOL plasma the temperature according to the ion energies, which allowed estimations of recycling at the high  $T_s$ . Over the whole vessel the conservation of particle number for each kind  $m$ , energy and momentum is observed.

With the new models three benchmark calculations of full ITER H-mode ELM-free discharge have been performed for auxiliary heating by a 1 MeV D-beam of power 80, 96 and 144 MW

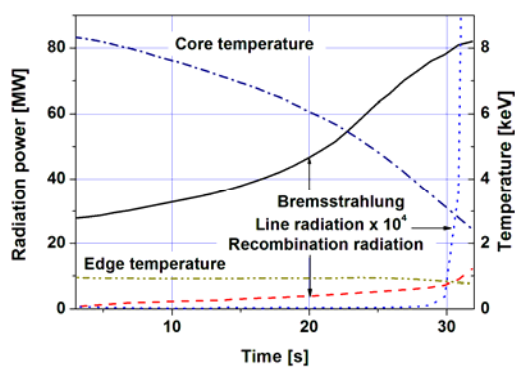


FIG. 8. Radiation losses and plasma temperatures obtained with TOKES, 80 MW heating.

and fuelling by pellets simulated homogeneously spreading 1 eV D-atoms over the confinement region. The plasma shape was fixed and the fusion reaction switched off. With 80 MW heating the discharge terminated after 33 s because of increasing radiation losses. Fig. 7 demonstrates the evolution of radiation power and plasma temperature. The main losses are due to bremsstrahlung. In the end phase the beam is mainly stopped at the plasma periphery and cannot therefore prevent the radiation collapse. For 96 and 144 MW heating, after about 20 s a steady state is reached. Table 1 shows some results of the steady state discharges. BP is the

beam power. Bremsstrahlung (B) always dominates over recombination (R)- and line (L) radiation.  $n_D$ ,  $T_{core}$  and  $T_{edge}$  are averaged over plasma volume. The edge temperature ( $T_{edge}$ ) is above 1 keV, which causes substantial impurity influxes by sputtering. The role of SOL in stopping of lost D-ions is small: their inflow ( $\Gamma_{SOL}$ ) is much larger than the atom outflow to the wall after charge-exchange collisions with SOL neutrals ( $\Delta\Gamma_{SOL}$ ).

**Table 1: Calculated steady state parameters of deuterium species**

BP MW	B MW	R MW	L W	$n_D$ $10^{20} \text{ m}^{-3}$	$T_{core}$ keV	$T_{edge}$ keV	$\Gamma_{SOL/D}$ $10^{20} \text{ s}^{-1}$	$\Delta\Gamma_{SOL/D}$ $10^{20} \text{ s}^{-1}$
96	21	4.7	11	1.1	10.5	1.07	103	0.12
144	8.5	0.31	3	0.65	18.5	1.54	103	0.06

Besides the plasma issues, in TOKES the poloidal field (PF) in the entire vessel is essential, because it determines at each time step the shape of confined plasma. PF is described with the poloidal magnetic flux  $w(\mathbf{p})$ , where the point  $\mathbf{p} = (r, z)$ , with  $r$  and  $z$  major cylindrical coordinates. The PF coil currents  $I_n$  are obtained using the plasma currents  $I_i$ . It is to note that if  $I_n$  would be fixed but  $I_i$  not, the plasma boundary can touch the wall in a few time steps, which is not desirable. Therefore to keep the plasma off the wall the updating of  $I_n$  is dynamically done [10]. The following control scheme is implemented: 1) fixed positions  $\mathbf{p}_{x0}$  and  $\mathbf{p}_{x1}$  for two x-points are chosen as expected in ITER; 2) the confined plasma is bounded by the separatrix magnetic surface  $w(\mathbf{p}) = w_{x0} \equiv w(\mathbf{p}_{x0})$ ; 3) another separatrix  $w(\mathbf{p}) = w_{x1} \equiv w(\mathbf{p}_{x1})$  locates outside the plasma and a small difference  $\Delta w = w_{x0} - w_{x1}$  is fixed; 4) some fixed positions  $\mathbf{p}_{cj}$  for several points near the vessel surface are chosen where the plasma can touch the wall most probably; 5) the point  $\mathbf{p}_{cjmax}$  of maximum value of  $w(\mathbf{p}_{cj})$  obtained with the available  $I_i$  and previous  $I_n$  is used for calculation of new  $I_n$  from the condition  $w(\mathbf{p}_{imax}) = w_{x1}$ . Thus the code tries to keep the outer separatrix  $w(\mathbf{p}) = w_{x1}$  near the wall and therefore the plasma at some distance from the wall.

Here the evaluation by TOKES of the currents  $I_n$  at total plasma current 15 MA is demonstrated, assuming the plasma conductivity  $\sigma(w)$  be linearly dependent on  $w$  (the bootstrap current is ignored). At fixed  $\mathbf{p}_{xm}$ ,  $\mathbf{p}_{cj}$  and  $\mathbf{P}_n$ , the ratio  $h = \sigma(w_{max})/\sigma(w_{x0})$  determines the state completely. In Figs. 9 to 12 the calculated plasma configurations at different plasma current profiles are shown. As we see, the separatrix that crosses the x-point  $x_0$  always locates not appropriately in the outer divertor leg Therefore additional PF coil near the divertor leg is necessary for the required shift of SSP.

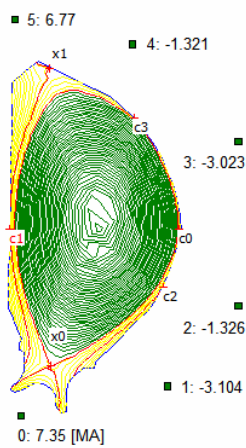


Fig. 9  $h = 4.13$

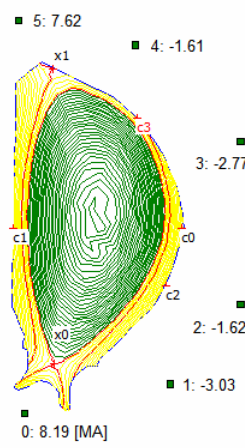


Fig. 10  $h = 1$

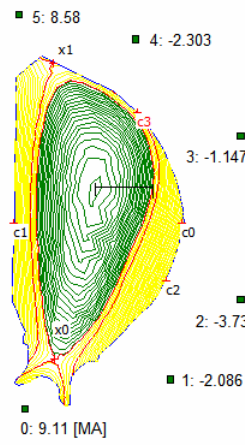


Fig. 11  $h = 0.39$

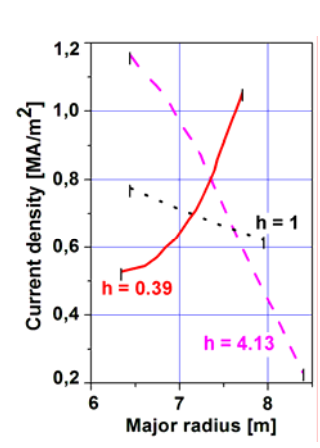


Fig. 12 Plasma currents

## 5. Conclusions

A good agreement between the measured and the calculated by FOREV dependences of the absorbed energy density on the incident heat load provide reliable validation of the carbon plasma shield simulation. High carbon plasma shield densities of  $10^{23}$ - $10^{24}$  m<sup>-3</sup> predicted in the simulations for ELM-produced shields has been proved in MK-200UG experiments. On the basis of these experiments and simulations, significant plasma contamination is expected for ITER transients at the target heat deposition above 0.5 MJ/m<sup>2</sup>, which corresponds to the vaporization threshold.

The TOKES modelled the cases without ELMs and that with ELMs of given energy, for the Be-C-W and Be-W walls of ITER design. With B-C-W wall, the scattered atoms have significant chances to strike secondarily the dome and thus produce sputtered W-atoms even with the CFC wall at the separatrix strike point (SSP). The ELMs may cause untimely discharge interruption, which corresponds to the vaporization onset at SSP. Replacing CFC by W resulted in rather fast termination of even ELM-free discharge caused by drastic increase of tungsten density in the confinement region. The obtained results provide useful benchmarks of tokamak simulations, but more work is needed for further development of TOKES in order to reach reliable integrated modelling.

## Acknowledgements

This work, supported by the European Communities under the EFDA contract TCN/350-02 of Association between EURATOM and Forschungszentrum Karlsruhe, was carried out within the framework of the European Fusion Development Agreement. The views and opinions expressed herein do not necessarily reflect those of the European Commission.

## References

- [1] FEDERICI, G., et al, Plasma Phys. Control. Fusion 45 (2003) 1523.
- [2] LOARTE, A., et al., Proc. 20<sup>th</sup> IAEA Conference, 2004 Vilamoura Portugal.
- [3] SAFRONOV V.M. et al., "Evaporation and vapor shielding of CFC targets exposed to plasma heat fluxes relevant to ITER ELMs", 13<sup>th</sup> Intern. Conf. on Fusion Reactor Materials, Nice, France, Dec. 2007, to be published in J. Nucl. Mat.
- [4] PESTCHANYI S., LANDMAN I.S., "Simulation of carbon plasma shielding efficiency during ELMs", 18<sup>th</sup> Plasma Surface Interaction Conference, Toledo, Spain, May 2008, paper P1-97.
- [5] LANDMAN I.S., JANESCHITZ G., "Contamination of ITER Core by Impurities of Tungsten and Carbon", 8<sup>th</sup> Intern. Symposium on Fus. Nucl. Techn., Heidelberg, Germany, Sept. 2007, to be published in Fus. Eng. Design.
- [6] LANDMAN I.S., JANESCHITZ G., "Modelling of radiation impact on ITER beryllium wall", 13<sup>th</sup> Intern. Conf. on Fusion Reactor Materials, Nice, France, Dec. 2007, to be published in J. Nucl. Mat.
- [7] DERE K.P., A&A 466 (2007) 771-792.
- [8] RALCHENKO YU. et al. NIST Atomic Spectra Database: <http://physics.nist.gov/asd3>.
- [9] LANDMAN I.S., JANESCHITZ G., "Modelling of SOL transport and radiation losses for ITER with the integrated tokamak code TOKES", 18<sup>th</sup> Plasma Surface Interaction Conference, Toledo, Spain, May 2008, Paper P1-98.
- [10] LANDMAN I.S., JANESCHITZ G., "Calculation of Poloidal Magnetic Field in Tokamak Code TOKES", 35<sup>th</sup> EPS Conf., Crete, Greek, June 2008, to be issued on CD.